Proceedings of MARTEC 2010
The International Conference on Marine Technology
11-12 December 2010, BUET, Dhaka, Bangladesh

DRAG ANALYSIS OF DIFFERENT SHIP MODELS USING COMPUTATIONAL FLUID DYNAMICS TOOLS

Salina Aktar [1], Goutam Kumar Saha[2] and Md. Abdul Alim [3]

[1]Department of Natural Science
Stamford University
51, Siddeswari, Dhaka, Bangladesh
E-mail: salina854@gmail.com

[2]Department of Naval Architecture and Marine Engineering
Bangladesh University of Engineering and Technology , Dhaka-1000, Bangladesh
Email: goutamkumar@name.buet.ac.bd

[3]Department of Mathematics
Bangladesh University of Engineering and Technology , Dhaka-1000, Bangladesh
Email: maalim@math.buet.ac.bd

ABSTRACT

Drag analysis based on CFD (computational Fluid Dynamics) simulation has become a decisive factor in the development of new, economically efficient and environment friendly ship hull forms. In this research work three-dimensional Finite Volume Method has been applied to determine the drag coefficient. The numerical solutions of the governing equations have been obtained using commercial CFD software package FLUENT 6.3. Two conventional models namely Wigely and Series 60 are simulated to compute drag coefficient at different Froude number in case of steady turbulent. Two turbulence models, namely, Standard k-ε, and Shear stress transport (SST) k-ω are used to analyze turbulent flow. Velocity vectors as well as contour of pressure distribution have also been displayed graphically. The computed results show good agreement with the experimental measurements/numerical results obtained by other researchers.

Keywords: *Drag co-efficient, Viscous drag co-efficient, Wave drag coefficient, Froude number, Total Pressure , Velocity vectors.*

1. INTRODUCTION

One of the most active fields of ship hydrodynamics research today is the development of methods for computing the drag coefficient of the steady viscous flow with free surface around a ship hull. In these days with the development of new numerical tools, the advances in computer technology and the increase capability of data processing, Computational Fluid Dynamic (CFD) has made remarkable progress and allowed good results to be obtained. The interest and demand of the industry to implement new methods is one of the most important reasons that influence the development of CFD. In ship hydrodynamics, drag is also being named as "resistance".

It is vital to define the hydrodynamic performance of the hull, to calculate the engine power, capable to overcome the hydrodynamic resistance produced by the interaction of the hull with the flow. CFD allows ship designers to create a computer-generated model of a ship and then test the ship at various speeds in a simulated environment. The result from the CFD simulations is necessary to understand the complicated flow characteristics for an optimal hull design, which includes a low drag and high propulsive efficiency. This allows designers to determine if the total resistance of the ship is at an acceptable level from a financial standpoint as well as a physical standpoint.

The financial perspective relates to the cost of the engine and the fuel that the engine consumes in order to meet the ship's mission requirements.

There have been some experimental works on drag characteristics around the ship models available for validation of CFD. Sangseon [1] and Sakamoto *et al* [2] made an extensive review on various types resistance for the Wigley parabolic hull based on ITTC 1957 Model-Ship Correlation Line and using RANS(Reynolds-Averaged-Navier-Stokes) simulation. Fonfach *et al* [3] used Series 60 model on drag calculation by CFD code. Gray[4] investigated frictional resistance using another type of ship model. Previously one research work by Banawan *et al* [5] and one conference by Ozdemir *et al*[6] were presented for the computational analysis flow around ships. Computation of drag coefficient using turbulent model on RANS simulation were described by Repetto [7] and Senocak *et al*[8].

The computed results has been compared with other CFD method named Boundary Element Method (BEM) from Saha[9]. The two models most used in CFD to solve the turbulent phenomena, are the Standard k-ε model and the Shear Stress

Transport(SST) k-ω model have been studied in [10,12].

2. MATHEMATICAL MODEL

Total drag coefficient is normally broken down into a Froude number dependent component-wave drag co-efficient (residuary drag co-efficient) and a Reynolds number dependent component-viscous drag co-efficient (frictional drag co-efficient).

The bracketed names give an alternative breakdown:

Total drag coefficient (C_d)

= Wave drag co-efficient (C_w) +

Viscous drag co-efficient (C_v)

= Residuary drag co-efficient (C_r) +

Frictional drag co-efficient(C_F)

The turbulent flow around hull including the free surface is computed using the Reynolds-averaged Navier–Stokes (RANS) equations for a three-dimensional steady, incompressible and viscous turbulent flow. Both air and water are considered as a single fluid with variable properties. Two turbulent models namely the Standard k- ε and Shear Stress Transport k-ω are used in this category.

2.1 Governing Ship Flow Equations

The coordinate system (x, y, z) for calculating the viscous drag and the wave making drag is defined to represent the flow patterns around hull form as positive x in the opposite flow direction, positive y in port side and positive z upward where the origin at the aft perpendicular of the hull form, as shown in Fig.1.

Figure 1: Co-ordinate system

2.1.1Governing Equations of Fluent Model

Continuity equation:

$$\frac{\partial u_i}{\partial x_i} = 0 \qquad (1)$$

Momentum transport equation:

$$u_i \frac{\partial u_i}{\partial x_i} = -\frac{1}{\rho}\frac{\partial p}{\partial x_i} + \frac{\partial}{\partial x_i}\left[\upsilon\left(\frac{\partial u_i}{\partial x_j} + \frac{\partial u_j}{\partial x_i}\right)\right] + \frac{\partial}{\partial x_j}\left(-\overline{u_i' u_j'}\right) \qquad (2)$$

$$-\overline{u_i' u_j'} = \upsilon_t\left(\frac{\partial u_i}{\partial x_j} + \frac{\partial u_j}{\partial x_i}\right) - \frac{2}{3}k\delta_{ij} \qquad (3)$$

Turbulent Model Equations:

a) Standard k-ε model

The standard $k-\varepsilon$ model is a semi-empirical model based on model transport equations for the turbulence kinetic energy *k* and its dissipation rate ε The model transport equation for *k* is derived from the exact equation, while the model transport equation for ε was obtained using physical reasoning and bears little resemblance to its mathematically exact counterpart.

In the derivation of the $k-\varepsilon$ model, it was assumed that the flow is fully turbulent, and the effects of molecular viscosity are negligible. The standard $k-\varepsilon$ model is therefore valid only for fully turbulent flows.

Transport equations for the Standard *k-ε* model are given by:

$$\rho u_i \frac{\partial k_j}{\partial x_i} = \frac{\partial}{\partial x_j}\left[\left(\mu + \frac{\mu_t}{\sigma_k}\right)\frac{\partial \varepsilon}{\partial x_j}\right] + G_k + G_b - \rho\varepsilon - Y_M$$

$$\rho u_i \frac{\partial \varepsilon_j}{\partial x_i} = \frac{\partial}{\partial x_j}\left[\left(\mu + \frac{\mu_t}{\sigma_\varepsilon}\right)\frac{\partial \varepsilon}{\partial x_j}\right] + C_{1\varepsilon}\frac{\varepsilon}{k}\left(G_k + C_{3\varepsilon}G_b\right) - C_{2\varepsilon}\rho\frac{\varepsilon^2}{k}$$

In these equations G_k represents the generation of turbulent kinetic energy due to mean velocity gradients, G_b is the generation of turbulent kinetic energy due to buoyancy, Y_m represents the contribution of the fluctuating dilation in compressible turbulence to the overall dissipation.

Here $C_{1\varepsilon}$, $C_{2\varepsilon}$ and $C_{3\varepsilon}$ are set equal to 1.44, 1.92 and 0.09, respectively. σ_k=1.0 and σ_ε=1.3 are the turbulent Prandtl numbers for k and ε.

b) The Shear –Stress Transport (SST) k-ω Model

The SST *k-ω* turbulence model is a conglomeration of the robust and accurate formulation of the Standard *k-ω* model in the near-wall region, with the Standard *k-ε* in the far field. The SST *k-ω* is more accurate and reliable for a wider class of flows than the Standard *k-ω*, including adverse pressure gradient flows.

Transport equations for the SST *k-ω* model are given by:

$$\frac{\partial}{\partial t}(\rho k) + \frac{\partial}{\partial x_i}(\rho k u_i) = \frac{\partial}{\partial x_j}\left(\Gamma_k \frac{\partial k}{\partial x_j}\right) + G_k - Y_k + S_k$$

$$\frac{\partial}{\partial t}(\rho\omega) + \frac{\partial}{\partial x_i}(\rho\omega u_i) = \frac{\partial}{\partial x_j}\left(\Gamma_\omega \frac{\partial \omega}{\partial x_j}\right) + G_\omega - Y_\omega + D_\omega + S_\omega$$

In these equations, G_k represents the generation of turbulence kinetic energy due to mean velocity

gradients, G_ω represents the generation of ω, Γ_k and Γ_ω represent the effective diffusivity of k and ω, respectively, Y_k and Y_ω represent the dissipation of k and ω due to turbulence, D_ω represents the cross-diffusion term, S_k and S_ω are user-defined source terms. The constants applied in the high Reynolds number form of the SST *k*-ω turbulence model are equal to:

$\sigma_{k.1}$=1.176, $\sigma_{\omega.1}$ =2.0, $\sigma_{k,2}$=1.0, $\sigma_{\omega.2}$ =1.168, α_1=0.31,

$\beta_{i,1}$=0.075, $\beta_{i,2}$=0.0828, k=0.41.

2.1.2 Governing Viscous Drag Equations

Typically the friction drag coefficient is predicted using the ITTC'57 ship –model correlation line or some similar formulation.

Frictional drag coefficient $C_F = \dfrac{C_f}{0.5\rho V^2 S}$ where C_f is co-efficient of friction and $C_f = \dfrac{0.075}{\left(\log_{10} R_n - 2\right)^2}$

2.1.3 Governing Equations of Wave Making Drag

Continuity equation:

$$\nabla^2 \phi = \frac{\partial^2 \phi}{\partial x^2} + \frac{\partial^2 \phi}{\partial y^2} + \frac{\partial^2 \phi}{\partial z^2} = 0 \qquad (4)$$

Water-surface condition:

$$\frac{1}{2} \nabla \phi \nabla \left(\nabla \phi \right)^2 + g \phi_z = 0 \qquad (5)$$

Ship hull surface condition:

$$\vec{n}.\nabla\phi = 0 \qquad (6)$$

Free surface condition: The kinematic and dynamic boundary conditions on the free surface:

$$\phi_x \zeta_x + \phi_y \zeta_y - \phi_z = 0 \text{ at } z = \zeta \qquad (7)$$

$$g\zeta + \frac{1}{2}\left[\nabla\phi.\nabla\phi - U^2\right] = 0 \text{ at } z = \zeta \qquad (8)$$

Pressure on the hull surface by Bernoulli's equation:

$$p - p_\infty = \frac{1}{2}\rho\left(U^2 - \nabla\phi.\nabla\phi\right) - \rho g z \qquad (9)$$

Hydrodynamic force in the x-direction:

$$R_w = -\int_{S+S'} \left(p - p_\infty\right) n_x dS \qquad (10)$$

$S \rightarrow$ Mean wetted surface, $S' \rightarrow$ Fluctuating part

Wave making drag $C_w = \dfrac{R_w}{0.5\rho V^2 S}$

3. COMPUTATIONAL METHOD

3.1 Computational Method for Viscous Drag

To solve the governing equations, the fluid domain is subdivided into a finite number of cells and these equations are changed into algebraic form via discretisation process. Finite volume method is used for the discretisation. The convective terms are discretised using Second Order Upwind scheme and the diffusion terms by central- difference scheme. The coupling between the pressure and velocity fields was achieved using SIMPLE (Semi-Implicit Methods for Pressure- Linked Equation) algorithm.

To solve the governing equations, the fluid domain is subdivided into a finite number of cells and these equations are changed into algebraic form via discretisation process. Finite volume method is used for the discretisation. The convective terms are discretised using Second Order Upwind scheme and the diffusion terms by central- difference scheme. The coupling between the pressure and velocity fields was achieved using SIMPLE (Semi-Implicit Methods for Pressure- Linked Equation) algorithm.

3.2 Computational Method for Wave Making Drag

The computational domain "triad" is subdivided into two numerical grids; the numerical grid on the ship hull surface and the numerical grid on the water surface belong to the ship hull. The flow is superimposed from point sources located near to the patch centers and the boundary conditions are satisfied in the average over surface "patches".

During the iterations the non-linear free surface boundary condition is applied. The numerical grid on the water surface is updated with respect to the calculated wave heights and the calculated waterline. A convergence has been achieved, if the changes of the calculated deformation of the free water surface and the calculated wave making resistance are less than a certain criteria for each one.

4. COMPUTATIONAL DOMAIN AND BOUNDARY CONDITION

The ship model used for this study is Wigley parabolic and Series 60, which are standard for ship-hydrodynamics research, and are chosen because these are used by ITTC research program. Two types of hull modes used for the experimental and computational test are, given bellow, and the longitudinal profiles of the 3D model are shown in Figure 2 and 3. The principal particulars of Wigley and Series 60 hull are described in Table 1.

Figure 3: Wigley hull model

Figure 3: Hull of Series 60 model

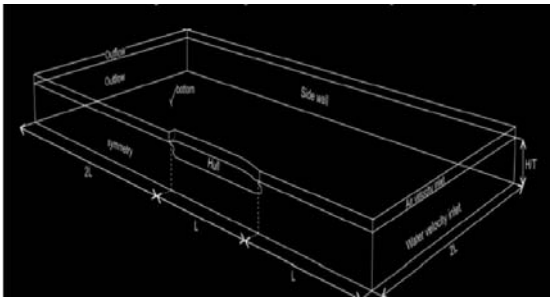

Figure. 4. Schematic diagram of the flow field around hull with boundary condition

Table 1: Principal particulars of Wigley and Series 60 model

Dimension	Wigley	Series60
Length Between Perpendicular [L_{PP}]	1.00[m]	1.00[m]
Breadth [B]	0.10[m]	0.133[m]
Draft [T]	0.0625[m]	0.053[m]
Block Coefficient [C_B]	0.44	0.60
Wetted surface area	0.135[m^2]	0.168[m^2]

The boundary condition was employed to simulate the condition on the towing tank. At the inlet a uniform flow is given. The free surface elevation was fixed at the inlet and at the outlet a hydrostatic pressure outlet boundary condition was used downstream; the hydrostatic pressure at the outlet was calculated assuming an undisturbed free surface. Smooth walls with a free-slip condition were assumed for the top, floor and the sidewall. Smooth walls with a non-slip condition (u, v, w = 0) were assumed in the entire hull.

The water condition was modeled as in the experimental test, which means fresh water at 100 Celsius , density = 1000 kg/m3, dynamic viscosity = 0.0008 kg/m-s, thermal conductivity = 0.677 w/m-k.

4. GRID GENERATION AND SIMULATION CRITERIA

In this study, 3D unstructured tetrahedral grids are constructed around the Wigley parabolic and Series 60 hull. Unstructured grid of 224189 mixed cells with 49483 nodes is constructed on the surface of Wigley model which are shown in Figure 4(a) and 4(b). Figure 5(a) and 5(b) shows the same pattern of grid of 1018918 mixed cells with 194443 nodes for the model Series 60.

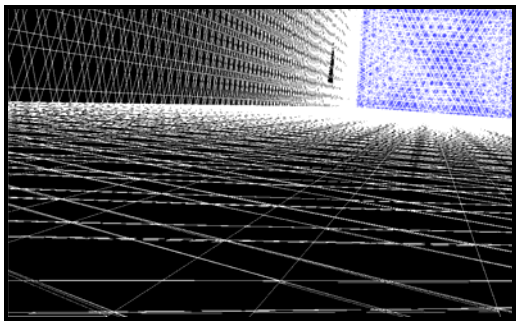

(a)

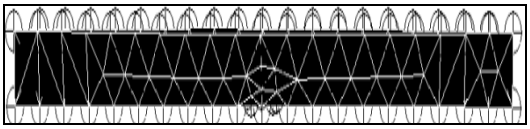

(b)

Figure 5: (a) Unstructured grid flow domain around and (b) Enlarged view of grid around the hull of wigley model

It is ensured that the computation domain and the number of grids are sufficient enough to calculate the drag coefficient on the hull accurately. In external flow simulations using Standard k-ε and SST k-ω the computational grid should be in such a way that sufficient number of grid points are within the turbulent sub-layer of the ensuing boundary layer. Unstructured tetrahedral grid is chosen because it is easily adjustable to complex geometry.

Plotting the flowing parameters against the number of iteration assessed convergence: Residuals for mass, momentum and turbulence (target criteria = 1E-3) and Drag forces (X directions). The maximum number of iterations was equal to 500. However, if the convergence criteria are reached for all residuals, the simulation was stopped before reaching 500 iterations.

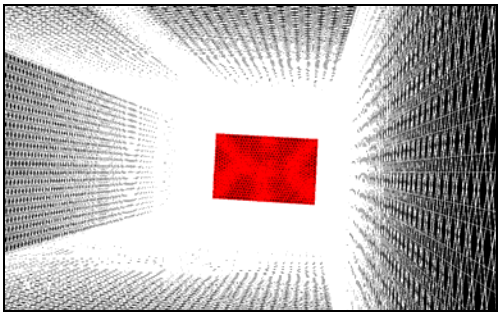

(a)

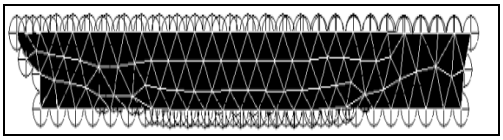

(b)

Figure 6.(a) Unstructured grid flow domain around and (b) Enlarged view of grid around the hull of series 60 model

6. RESULTS AND DISCUSSION

The computation of viscous (C_v), wave (C_w) and total (Cd) drag coefficient by standard k-ε (SKE) both for model wigley and series 60 at various Froude number has been showed in Table 2. In Figure 8(a) and (b) we see that with the increasing values of F_n, at first C_w and C_d increases significantly and then decreases whereas C_v decreases frequently. Different Froude number [0.173, 2.05, 269, 0.355, and 0.476] has been taken because wave making drag at these Froude number are high that are hump positions.

To compare and validate the numerical results, use have been made with another numerical named BEM[9] and experimental result [3] for Series 60 hull and also computed (SST) with another numerical result named BEM[9] for Wigley hull .

Table 2:Computed value of C_d, C_V and C_W of Wigley hull

Fn	$C_d \times 10^{-2}$	$C_v \times 10^{-3}$	$C_w \times 10^{-2}$
0.173	3.9	1.30	3.7
0.205	4.6	0.87	4.5
0.269	6.5	0.47	6.4
0.355	7.2	0.25	7.1
0.476	6.9	0.13	6.7

Table 3: Computed value of C_d, C_V and C_W of Series 60 hull

Fn	$Cd \times 10^{-2}$	$C_v \times 10^{-3}$	$C_w \times 10^{-2}$
0.173	12.6	8.25	11.7
0.205	30.8	5.65	30.2
0.269	90.75	3.08	90.4
0.355	75.6	5.97	75.0
0.476	85.1	8.72	84.2

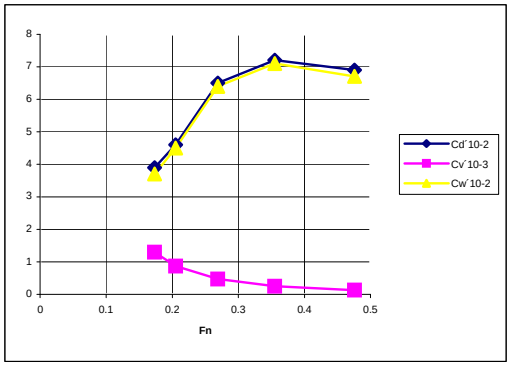

(a)

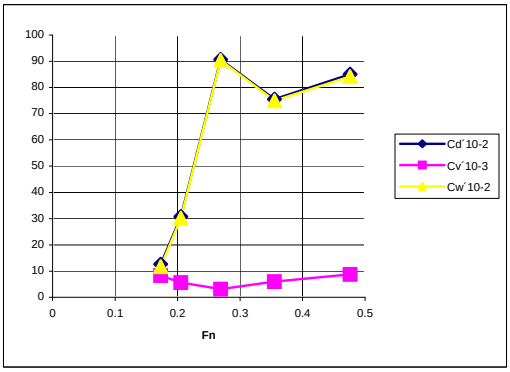

(b)

Figure 8. Fn vs various drag coefficient of (a) wigley hull (b) series 60 hull.

Table 4: Comparison of computed C_d by SKE, SST and BEM method for Wigley hull

Fn	SKE	SST	BEM
0.173	3.9×10^{-2}	6.1×10^{-2}	5.2×10^{-2}
0.205	4.6×10^{-2}	6.0×10^{-2}	3.9×10^{-2}
0.269	6.5×10^{-2}	5.8×10^{-2}	8.2×10^{-2}
0.355	7.2×10^{-2}	5.6×10^{-2}	3.5×10^{-2}
0.476	6.9×10^{-2}	5.4×10^{-2}	19.1×10^{-2}

Table 5: Comparison of computed C_d with BEM method and Experimental result for series 60 hull

Fn	SKE	BEM	Exp.
0.173	12.6×10^{-2}	12.1×10^{-2}	10.07×10^{-2}
0.205	30.8×10^{-2}	22.5×10^{-2}	44.2×10^{-2}
0.269	90.7×10^{-2}	39.1×10^{-2}	102.06×10^{-2}
0.355	87.6×10^{-2}	32.6×10^{-2}	64.97×10^{-2}
0.476	85.1×10^{-2}	606×10^{-2}	

From Table 4 it is seen that the computed values by SKE and SST agrees well with another computed result by BEM [9] for Wigley hull. The difference between the SKE and SST by 32% where as it is 30% for BEM method. As can be seen that results obtained from SKE are in good agreement with experimental data. From Table 5 for the Series 60 hull it is also seen that difference between the computed (SKE) and BEM method is 27% whereas it is 2.51%from the experimental [3] result. From both of the Table 2 and 3 the computed value has a nice agreement with the BEM and experimental result.

Drag convergence history is shown in Figure 9. Contours of total pressure around Wigley and Series 60 are shown in Figure 10(a) and 10(b) respectively. Figure 11(a) and 11(b) show the plot of velocity vectors around the hull. The path lines around the hulls are shown in Figures 12(a) and 12(b).

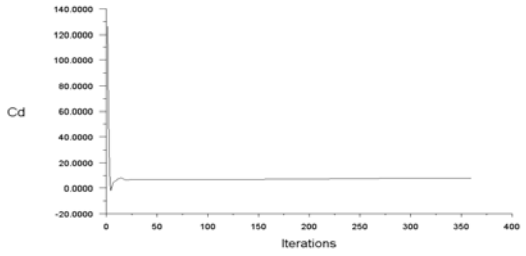

Figure 9: Drag convergence history

7. CONCLUSION

In this research work we have obtained drag co-efficient of two models: Wigley and Series60 by using CFD code FLUENT. We also compared numerical results computed by SKE and SST models of FLUENT and compared with BEM and experimental values. From comparative values it is seen that total drag coefficient for FLUENT model, BEM and experimental shows a good agreement in the range of Froude number from 0.2 to 0.3. Whenever the range exceeds 0.3 there occur a large variation among the computed, BEM and experimental result. This variation can be minimized by decreasing the the mesh size, refining mesh etc.

Based on the results of a CFD simulation, a ship designer can choose optimum speed with minimum power annd then proceed to a model test for experimental result.

8. ACKNOWLEDGMENTS

The authors thank MARTEC 2010 conference organizer for giving us the opportunity to present the research work.

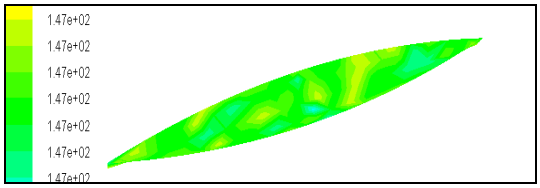

(a)

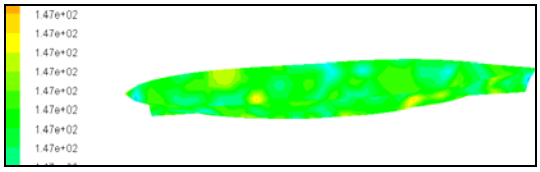

(b)

Figure 10: Plot of total pressure of (a) Wigley and (b) Series 60 hull

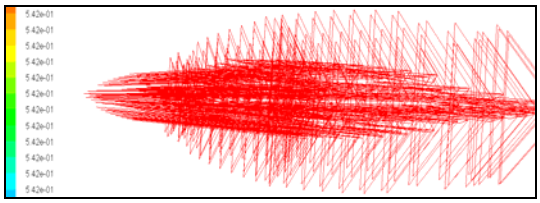

(a)

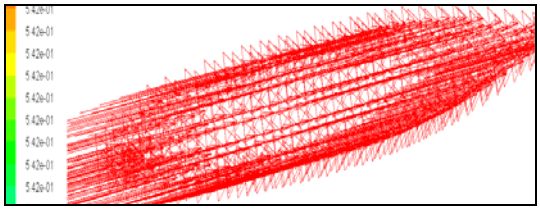

(b)

Figure 11: Plot of velocity vectors around (a) Wigley and (b) Series 60 hull

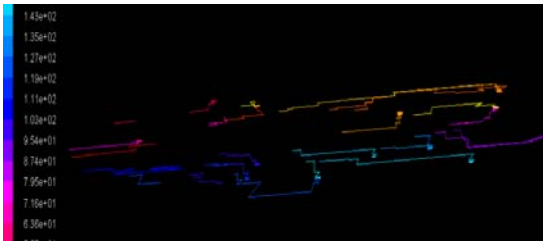

(a)

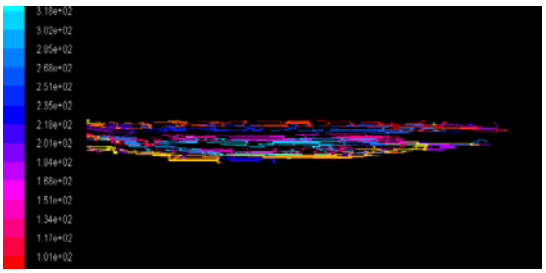

(b)

Figure 11: Plot of path lines around (a) Wigley and (b) Series 60 hull

9. REFERENCES

[1] Sangseon, J., Study of Total and Viscous Resistance for The Wigley Parabolic Ship Form, *Iowa Institute of Hydraulic Research, IIHR Report No*.261. (1983).

[2] Sakamoto,N., Wilson,R.V and Stern,F., Reynolds-Averaged Navier-Stokes Simulations for High-Speed Wigley Hull in Deep and Shallow Water *Journal of Ship Research*, Vol. 51, No. 3, pp. 187–2003,September (2007)

[3] Fonfach, J. M. A. and Soares,. C. G, Improving The Resistance Of A Series 60 Vessel with a cfd code, *European Conference on Computational Fluid Dynamics,ECCOMAS CFD,J. C. F. Pereira and A. Sequeira (Eds),Lisbon, Portugal*, 14–17 June (2010).

[4] Gray, A. W., Preliminary Study on The Use of Computational Fluid Dynamics to Determine The Frictional Resistance of a Trimaran Ship, *M.S thesis, Department of Mechanical and Aerospace Engineering, West Virginia University, Morgantown*, USA, (2007).

[5] Banawan, A. A. and Ahmed, Y. M., Use of Computational Fluid Dynamics for The Calculation of Ship Résistance, and Its Variation with The Ship Hull Form Parameters, *Alexandria Engineering Journal*, Vol. 45, No.1, (2006)

[6] Ozdemir, Y. H., Bayraktar, S. and Yilmaz, T., Computational Investigation of A Hull, *2nd International Conference on Marine Research and Transportation, Ischia, Naples, Italy*, 28th-30th *June*, (2007).

[7] Repetto, R.A., Computation of Turbulent Free-Surface Flows Around Ships and Floating Bodies, *PhD. Thesis, Technical University Hamburg-Harburg, Argentina* (2001).

[8] Senocak,. I and Iaccarino,G, Progress towards RANS simulation of free-surface flow around modern ships,*Center for Turbulence Research Annual Research Briefs* (2005)

[9] Saha,G.K.,"Numerical optimization of ship hull forms from viewpoint of wave making resistance based on panel method" , *Ph.D Thesis, Yokohama National University,* Yokohama, Japan[2004]

[10] Mulvany, N. J., Chen, L., Tu, J. Y. and Anderson, B., Steady-State Evaluation of Two-Equation.RANS (Reynolds-averaged Navier Stokes) Turbulence Models for High-Reynolds Number Hydrodynamic Flow Simulations,. *Maritime Platforms Division, Defence Size and Technology Organization, Deparment of Defence, Australian Government* (2004)

[11] Versteeg, H.K. and Malalasekera, W., *An Introduction to Computational Fluid Dynamics, Longman Scientific & Technical,* England (1995).

[12] Hoffmann, K. A. and Chiang, S.T., Computational Fluid Dynamics (Third Edition), Vol. 2, Wichita KS: Engineering Educational System, (1998).

[13] http://www.cfdonline.com/Wiki/Turbulence_modeling